

Review

Spatiotemporal Patterns of the Application of Surface Urban Heat Island Intensity Calculation Methods

Jiyuan Zhang , Lili Tu * and Biao Shi

College of Resources and Environment, Anhui Agricultural University, Hefei 230036, China; zhangjiy@stu.ahau.edu.cn (J.Z.); 20720670@stu.ahau.edu.cn (B.S.)

* Correspondence: tulili@ahau.edu.cn

Abstract: Using the China National Knowledge Infrastructure (CNKI) and Web of Science (WoS) databases, 487 articles that used remote sensing methods to study the intensity of surface urban heat islands (SUHIs) over the past 20 years were obtained using keyword searches. A multidimensional analysis was conducted on these articles from the perspectives of the research methods used, spatiotemporal distribution characteristics of the research area, research development trends, and main challenges. The research found that (1) the growth trend of the various SUHI research methods over the years was similar to the overall trend in the number of publications, which has rapidly increased since 2009. (2) Among the SUHI research methods, temperature dichotomy is the most widely used worldwide; however, defining urban and rural areas is a main challenge. The Gaussian surface and local climate zoning methods have gradually emerged in recent years; however, owing to the limitations of the different urban development levels and scales, these methods require further improvement. (3) There are certain differences in the application of SUHI research methods between China and other countries.

Keywords: surface urban heat island; heat island intensity; land surface temperature; remote sensing; calculation method; spatiotemporal patterns



Citation: Zhang, J.; Tu, L.; Shi, B. Spatiotemporal Patterns of the Application of Surface Urban Heat Island Intensity Calculation Methods. *Atmosphere* **2023**, *14*, 1580. <https://doi.org/10.3390/atmos14101580>

Academic Editors: Francesca Despini, Sofia Costanzini and Matthew Eastin

Received: 18 August 2023
Revised: 2 October 2023
Accepted: 16 October 2023
Published: 19 October 2023



Copyright: © 2023 by the authors. Licensee MDPI, Basel, Switzerland. This article is an open access article distributed under the terms and conditions of the Creative Commons Attribution (CC BY) license (<https://creativecommons.org/licenses/by/4.0/>).

1. Introduction

Since the reform and opening up, the social economy has rapidly developed and urbanization has accelerated. The level of urbanization in China rose from 17.9% in 1978 to 52.6% in 2012. By 2020, it far exceeded the average standards of developing countries, reaching 63.89%. According to a United Nations estimate, the urbanization rate of developed countries will reach 86% by 2050 and China will reach 71.2% at that time. An increase in urbanization promotes economic development, improves living standards, and enhances human well-being. However, it also causes a series of urban diseases and exacerbates global warming and the urban heat island (UHI) effect. The UHI effect is a phenomenon characterized by higher urban temperatures than rural temperatures, which has serious implications of ecological problems; for example, extreme weather endangers human health at mid and low latitudes. To maintain sustainable development worldwide, it is important to investigate the UHI effect and measures to mitigate it.

An early study on the UHI effect at Howard noted that temperatures were higher in central London than in the suburbs in the early 19th century [1]. Since then, many studies have been conducted on urban heat island intensity (UHII) [2–4], drivers of the UHI effect [5,6], spatiotemporal evolution characteristics [7,8], and mitigation measures [9,10]. Currently, UHIs are divided into three categories: boundary layer heat islands (BLHIs), canopy layer heat islands (CLHIs), and surface urban heat islands (SUHIs). The BLHI and CLHI are components of atmospheric heat island research, which is primarily based on meteorological data and employs ground observations and numerical simulations [11]. A SUHI is the heat island expressed by the land surface temperature (LST), which is measured using thermal infrared (TIR) remote

sensing, and the thermal radiation information of an urban surface and its features can be timely and accurately obtained using satellite remote sensing technology, which has the advantages of a short cycle of data acquisition, wide coverage, and low acquisition cost. In 1972, Rao [12] first discovered the SUHI phenomenon in the eastern United States using satellites. Later, several academics conducted in-depth discussions on SUHIs and established many methods to study SUHI intensity (SUHII) [13–15]. This research compared and analyzed articles on SUHIs based on remote sensing methods over the past 20 years, aimed to understand the status of past research on SUHIs, and provides a reference for future research, which is of far-reaching significance to global sustainable development, research on climate change, and the mitigation of UHI effects.

2. Data Sources and Method

The China National Knowledge Infrastructure (CNKI) and Web of Science (WoS) were used as article search platforms. Conducting an advanced search in the CNKI database, the search topics were “urban heat island” and “heat island intensity”, the period was 2002–2021, and the journal sources were SCI, EI, core journals, and CSSCI. Thus, 649 articles were identified. According to WoS (Core Collection database), we searched “surface urban heat island” and “heat island intensity”, with the article type “Article” or “Review Article” and the period 2002–2021, and 945 articles were retrieved. The search results were screened manually to exclude conferences, newspapers, and irrelevant articles. Articles that did not use SUHII as the main research topic and remote sensing as the main research technique were excluded. Finally, 487 valuable articles were retrieved, of which 181 were retrieved from CNKI and 306 from WoS (Core Collection database). Further, we extracted the titles, posting times, research ranges, and topics of the articles.

3. Historical Trends

The number of publications reflects whether a field is active. Figure 1 shows the number of articles published on SUHI research from 2002 to 2021. It can be seen that SUHI research showed an overall upward trend over the last 20 years. It was in the early stages of development from 2002 to 2008 and rose sharply from 2009 to nearly five times the number of publications a year ago. The highest number of articles was issued in 2021, when the total number of articles reached 92. The increase in the number of publications was mainly due to the following reasons: First, in recent years, the frequent incidences of global warming, extreme drought, and heat waves have led scholars to focus on urban climate change and SUHI research [16]. It has been found that most countries in the world are facing increasing challenges in terms of livability [17]. It is critical to comprehend the drivers of SUHIs and develop mitigation strategies. Thus, an increasing number of scholars are interested in SUHIs, with a growing number of studies being published [18,19]. Second, the boundaries of urban, rural, and suburban areas are constantly changing because of the expansion of urban construction land and the interconversion of each land use type [20], necessitating further improvement in SUHII calculation methods [21,22]. Third, with the continuous progress in science and technology, especially the emergence of MODIS, Landsat, and Sentinel satellites, based on which satellite remote sensing data sources are continuously expanding and improving, the accuracy of LST retrieval has continuously improved, and SUHI research with LST as the main data source has substantially improved the efficiency and accuracy [23]. Several articles have reviewed and evaluated different sensors/satellites imagery used in SUHI research [18,24].

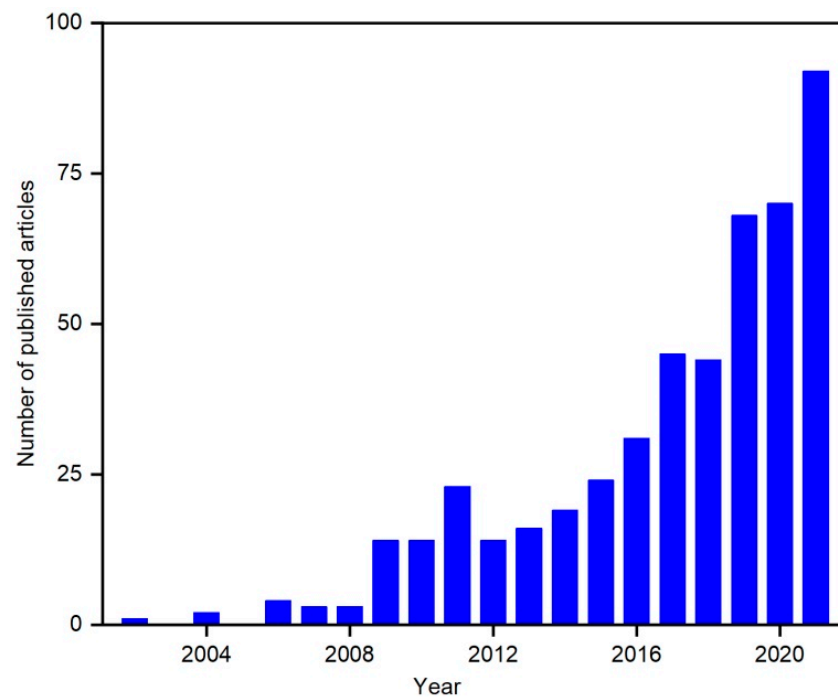


Figure 1. Number of published articles in each year.

4. Methods for Measuring SUHII

We further analyzed and summarized the SUHI methods, based on the research of Li [24], Budhiraja [25], and other academics [26,27], and classified the SUHI methods into four categories: temperature dichotomy method, LST/bright temperature (BT) grading method, Heat Island Index method, and statistical models. These four different types of methods are listed in Table 1.

Table 1. Classification of SUHII research methods based on remote sensing.

Type	Method	Illustration	References	Application Number
Temperature Dichotomy Method	Urban–Rural Method	Average LST difference between urban and rural areas by administrative boundaries.	Ren et al. [28]; Deng et al. [29]	59
		Average LST difference between new/old city and nonurban areas.	Gui et al. [30]; Wang et al. [8]	3
	Urban–Buffer Zone Method	Average LST difference between urban built-up areas and rural areas according to ISA, NDVI, OLS, LULC, SUE, etc.	Zhang et al. [31]; Chakraborty et al. [32]	58
		Difference between each pixel and the average LST in the study areas.	Wang et al. [33]	20
		Average LST difference between urban areas and the surrounding n km buffer. (Urban areas determined from NDVI, ISA, OLS, BI, etc.)	Clinton et al. [34]; Zhou et al. [6]	99

Table 1. Cont.

Type	Method	Illustration	References	Application Number
		Average LST difference between urban areas and the surrounding buffer zone that 50%, 100%, and 150% of urban areas are based on the using urban clustering algorithm.	Peng et al. [35]	16
	Urban–Field Method	Average LST difference between urban and field areas.	Ye et al. [36]	33
	Urban–Vegetation Method	Average LST difference between urban and vegetation areas.	Fang et al. [37]; Zhou et al. [38]	12
	Urban–Water Body Method	Average LST difference between urban and water body areas.	Gawuc et al. [39]	3
	Local Climate Zones (LCZs)	Average LST difference between LCZs and a particular LCZ (e.g., low vegetation type)	Zhang et al. [40]; Budhiraja et al. [25]	16
LST/BT Grading Method	—	Grading according to different periods of LST or BT images	Xiong et al. [41]; Huang et al. [42]	109
Heat Island Index	Urban Heat Island Ratio Index (URI)	Ratio of the UHI area to built-up area and assigned weights to characterize the SUHII	Xu et al. [43]	40
	Urban Thermal Field Variance Index (UTFVI)	Ratio of the difference between the LST of each pixel and the mean LST to the mean LST of the study areas	Chen et al. [44]	32
	Maximum Urban Heat Island Intensity (MUI) and Weighted Average Urban Heat Island Intensity (WAUI)	MUI refers to the difference between the maximum temperature in the urban areas and the minimum temperature in the suburbs. WAUI refers to the difference between the average LST and the proportion of the average LST in each class of areas of the city and the average LST in the suburbs	Zhang et al. [45]	5
Statistical Models	Gaussian Surface Model (GSM)	Fitting of the rural temperature image to a plane and then decreasing the rural temperature image from the original surface temperature image	Hu et al. [46]; Schwarz et al. [14]	16
	Kernel Convolution Method	Difference between the maximum and minimum values of the LST after processing according to the kernel convolution method	Weng et al. [47]	2

Table 1. Cont.

Type	Method	Illustration	References	Application Number
	Moran's I (MI) and Getis-Ord G_i^* (G_i^*)	Explains the spatial aggregation patterns of the SUHI at the overall and local spatial scales, respectively	Liu et al. [48]; Li et al. [49]	10
	Linear Relationship Between LST and ISA (or HIS)	Regression slope of the LST and ISA (or HIS) fit function is regarded as the SUHII	Li et al. [50]; Zhang et al. [51]	3

4.1. Temperature Dichotomy Method

The SUHII is defined as the difference in the LST between urban and nonurban areas (Equation (1)) [28,52]. The question of how to define urban and nonurban boundaries is a core issue for SUHIs because distinguishing between urban and nonurban areas using different methods can affect the results of studying the SUHII [53,54]. This weighty and difficult point has aroused intensive discussions among numerous academics, and the temperature dichotomy method has led to various calculation methods [55,56]. Based on the different types of land cover in a city, a series of methods are used to extract urban, rural, and field types. Next, the SUHII is obtained by calculating the average LST difference between urban and nonurban areas (LST of rural/field/vegetation/water body/surrounding buffer zones).

$$SUHI = LST_{urban} - LST_{non-urban} \quad (1)$$

where LST_{urban} refers to the average LST in urban areas, and $LST_{non-urban}$ refers to the average LST in nonurban areas.

An administrative boundary is an important unit of regional social and economic statistics, and it is used to divide urban and nonurban areas and to highlight the impact of human activities on the urban thermal environment. The level of urban development and construction can also be identified using built-up intensity (BI), impervious surface area (ISA) density, Normalized Difference Vegetation Index (NDVI), and nighttime light intensity data (such as DMSP/OLS), which can be distinguished from other areas based on these indicators [57,58]. Additionally, fields, vegetation, and water bodies can be used as representative pixels of nonurban areas [36,39,59], and the SUHII is obtained according to the LST difference between urban and nonurban areas. Although the above methods can clearly and quickly obtain the LST difference between urban and nonurban areas, there is a certain degree of subjectivity and a lack of uniform standards and systems in the definition of urban extent and the selection of rural or suburban pixels. This is because even if fields with small urban height differences, stable planting structures, and soil properties far from an urban center are selected, they cannot fully represent the characteristics and LST of nonurban areas. With rapid urbanization, construction land in different countries and regions is expanding significantly, different land types are transforming, and the boundary between urban and rural areas is gradually blurring. Consequently, defining urban and rural areas, selecting representative rural pixels, and choosing appropriate thresholds to make SUHIs comparable in different cities or at different stages remain hot topics for academic discussion [13]. Currently, research on SUHIs based on the local climate zones (LCZs) theory is gradually increasing [25,60,61]. For instance, some studies measured the SUHII of each LCZ as the LST difference between the item and the low vegetation type [62]. The advantage of the LCZs method is that it considers the influence of 3D urban building forms on the SUHI, which is more objective and scientific than previous studies that only considered the 2D layout of the city.

Peng et al. [35] defined urban areas based on a urban clustering algorithm, defined suburban areas as all nonurban pixels (excluding water pixels) within a ring around urban areas, and compared the heat island intensities of equal, smaller, and larger suburban areas (as 100%, 50%, and 150% of urban areas, respectively). Additionally, NDVI, ISA, BI, and other indicators can be used to determine urban areas, and the difference between the determined LST of urban areas and the average LST within the surrounding n km buffer zone was taken as the SUHII. The advantage of this type of method is that it can make the heat island intensity of different periods horizontally comparable; therefore, it is widely used in SUHII research, but its disadvantage is that it has not explored a universal buffer width for the time being. The question that needs to be considered is what buffer width should be chosen for different study areas to better analyze the SUHII. Chakraborty et al. [32] developed a simplified urban extent (SUE) algorithm, which has the advantage of automatically calculating the SUHII on a global scale and no need of dividing urban areas from nonurban areas by defining buffers, as it is based on cloud computing with big data and can minimize the differences in the SUHII due to urban–rural selection. However, this method requires the testing of multiple remote sensing datasets to ensure the accuracy of the algorithm.

4.2. LST/BT Grading Method

Among the 181 articles in the CNKI database, the most frequently used method was the LST/BT grading method, which classifies the SUHI using one or more LST (or BT) images and treats high-temperature areas as heat island areas. The division methods mainly include the mean value and standard deviation, natural breakpoint, and equal-interval methods [15]. Lu et al. [15] classified the urban LST in Beijing using five classification methods and investigated the robustness of the five classification methods in terms of defining urban heat island patches. The LST/BT grading method can accurately identify the distribution of the SUHI in the study area and visually compare the spatial and temporal evolutionary characteristics of the SUHI during different periods using thermal infrared images of different periods. However, it can only classify the study area into different temperature classes using a certain classification index and can quickly identify the distribution characteristics of heat island areas. If a comprehensive and detailed SUHII of the study area is required, it must be combined with the Heat Island Index for calculation. The Heat Island Index method is described in the following sections.

4.3. Heat Island Index

The Heat Island Index method includes the URI, UTFVI, MUI, and WAUI.

Xu et al. [43] introduced the URI (Equation (2)) in a quantitative study of the UHI changes in Xiamen City, which solved the problem of comparing the thermal infrared images from different periods. The URI is often combined with the LST/BT grading method, which has the advantage of reflecting changes in the SUHI in a more objective and quantitative manner. The equation can be expressed as:

$$URI = \frac{1}{100m} \sum_{i=1}^n w_i p_i \quad (2)$$

where m is the level of normalization, i is the LST grade of the urban area over the suburban area, n w_i is the number of grades of the urban area over the suburban area, is the weight value of class i , and p_i is the area percentage of class i .

The UTFVI [44] is used to quantitatively analyze the heat island effect, and it can clearly determine the range and location of the high- or low-temperature heat distribution in an image. It can be expressed as:

$$UTFVI = \frac{T - T_{mean}}{T_{mean}} \quad (3)$$

where T is the LST of a point in the city, and T_{mean} is the average LST of the urban area.

The MUI (Equation (4)) and WAUI (Equation (5)) are two important indicators for characterizing the SUHI [45]. One is the difference between the maximum and minimum LST values in the study area, and the other is calculated using the average temperature of the urban area as the base and utilizing the average temperature of each class area and its percentage. These can be expressed as:

$$MUI = T_{max} - T_{min} \quad (4)$$

where T_{max} is the maximum LST, and T_{min} is the minimum LST.

$$WAUI = (T1_{avg} - T0_{avg}) \times A1 + (T2_{avg} - T0_{avg}) \times A2 + (T3_{avg} - T0_{avg}) \times A3 \\ + (T4_{avg} - T0_{avg}) \times A4 + (T5_{avg} - T0_{avg}) \times A5 \quad (5)$$

where $T1_{avg}$ – $T5_{avg}$ are the LSTs from the high-temperature areas to the low-temperature areas, $T0_{avg}$ is the average LST of the urban area, and $A1$ – $A5$ are the percentages of the built-up areas from the high- to low-temperature areas.

4.4. Statistical Models

Many statistical models have been applied in SUHI studies [46,47,63]. The Gaussian surface model (GSM) performs well in quantifying the SUHI, and the spatial distribution of heat islands can be described using a Gaussian surface superimposed on a flat rural background. Compared with the traditional temperature dichotomy method, this method can reduce the uncertainty between urban and rural boundaries; however, the GSM is not suitable for the application of urban research in the form of multicore expansion construction and cannot adapt to the master planning requirements of polycentric development in many cities at this stage. The kernel convolution method was applied to the LST images and used to characterize the UHI effect [47]. Although it is efficient for characterizing continuous surface space temperature values, it is easily affected by missing values in the remote sensing images during processing. MI and G_i^* are measures of spatial autocorrelation [48]. The use of these two indicators enables the identification and agglomeration analysis of heat island ranges in the study area. However, the disadvantage is that they do not consider the influence of natural factors, such as topography and land use type. The kernel convolution model was applied to the LST images to characterize the UHI effect. However, it is susceptible to missing values in remote sensing images during processing; therefore, it is not widely used. Li et al. [50] indicated that the ISA can reflect the spatial pattern of the SUHI, and the relationship between the LST and ISA can be a powerful tool for quantifying the SUHI. Based on this, Li et al. proposed a method to study the slope of the linear regression function of the LST and ISA as the SUHI, which avoids bias because of the selection of urban and nonurban pixels and provides the possibility of a comparison between different SUHIs. Nevertheless, this method assumes that the LST increases with the ISA, but it is not applicable for desert cities because the relationship between the LST and ISA is not positively correlated, in addition to having a U-shaped structure [64].

5. Spatial and Temporal Distribution Characteristics of SUHI Research Methods

5.1. Analysis of Temporal Pattern of SUHI Research Methods

Figure 2 shows the results of the statistics on the number of new and accumulated applications of various SUHI research methods over the years according to the number of published articles per year.

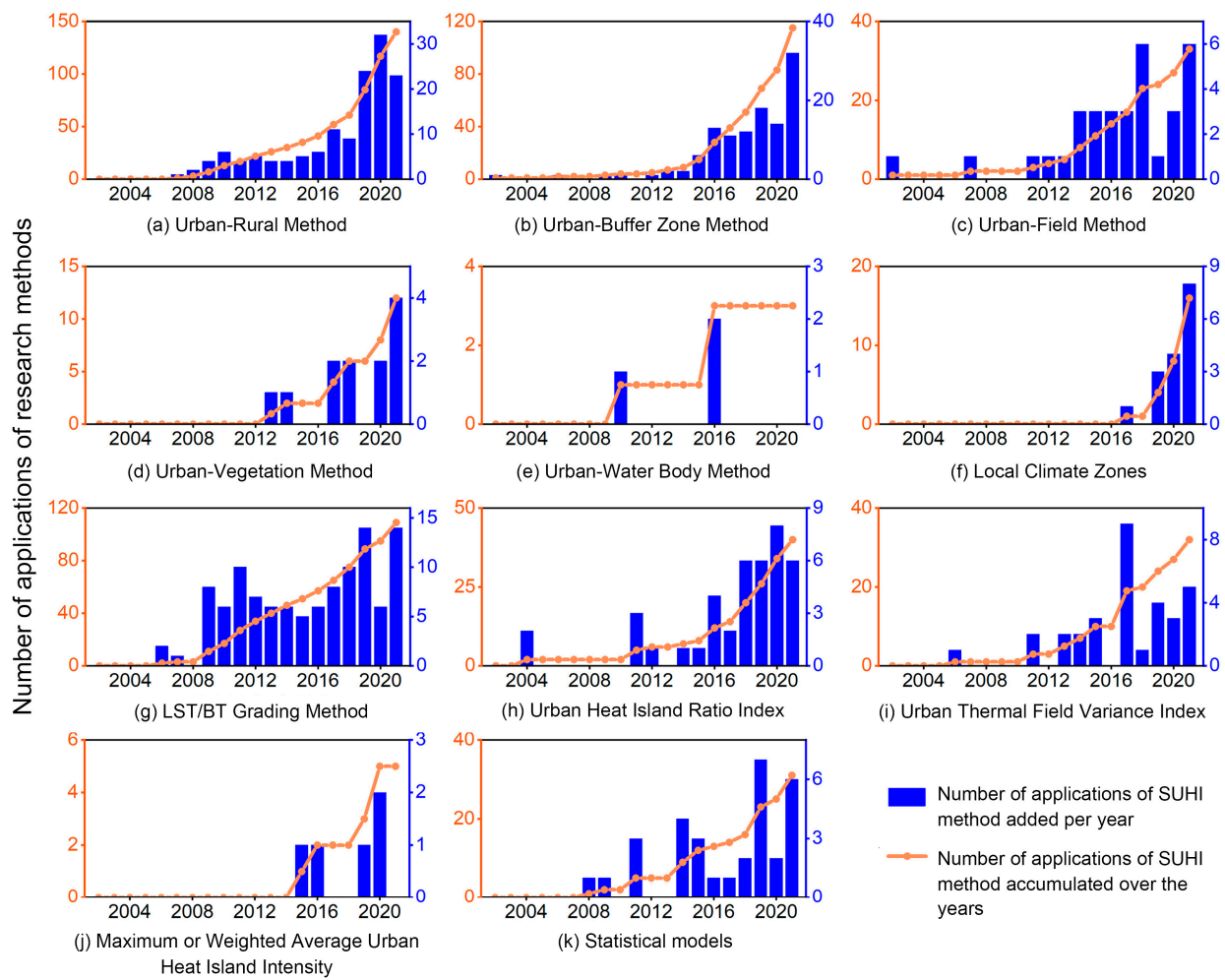


Figure 2. Number of new applications of the SUHI research methods added per year and accumulated over the years.

Overall, the urban–water body method and MUI/WAUI were applied less, and the growth trends of the SUHI research methods showed roughly the same trend as the overall number of published articles. In the early stages of the study period (2002–2008), the LST/BT grading method dominated the research method. In addition, the urban–rural, urban–field, URI, and UTFVI methods were applied to a smaller extent. During the middle stage (2009–2018), the application of the urban–rural, urban–buffer zone, urban–field, LST/BT grading method, URI, and UTFVI methods gradually increased, and the application of the temperature dichotomy method gradually matured. In 2015, Zhang et al. [45] calculated and analyzed the SUHII of Chengdu city using the MUI/WAUI, which was an earlier application of this index. In 2012, Stewart and Oke [65] analyzed a large number of UHI studies and proposed an LCZs system, indicating that the method can compensate for the shortcomings of the traditional temperature dichotomy method and clarify the correlation between urban morphology and temperature. Initially, it was often used to study local temperatures in cities. Since 2017, it has gradually been applied to SUHIs. In recent years (2019–2021), SUHI research has continued to increase, with the temperature dichotomy method, especially the urban–rural dichotomy, still leading in the frequency of application; further, the method has improved over time. It is worth noting that while the LST/BT grading method has been used 109 times in total, it has mostly been used for small-scale and single-city-wide research. A single LST retrieval method and heat island classification method cannot meet the needs of diverse cities on a large scale. If all of the cities included in the study were to choose different classification methods for heat island identification and classification, it would certainly add a lot of extra effort, making the method

much less useful. Therefore, as a result of the increased demand for research, the LST/BT grading methods' growth rates have slowed in recent years. In short, SUHI research methods have gradually evolved from single and simple to varied and detailed.

5.2. Analysis of the Spatial Pattern of SUHI Research Methods

The research methods for SUHI were widely applied, as shown in the 487 papers, of which 14 papers have a global scope of study, and most of the rest have national, city, and urban clusters as the scale of study. According to Figure 3, the distribution of SUHI studies in Asia is very large, particularly in China, which has far outpaced the literature (65.50%). India comes in second with 5.34%. The SUHI-related research in North America is mainly concentrated in the United States with a share of 4.11%. Some areas in these countries have been widely studied and discussed owing to recent high levels of urbanization or population explosions in recent years, and the UHI problem is prominent and significant. The correlation between the number of people (Asia > Africa > Europe > North America > South America > Oceania > Antarctica) and the number of SUHI studies from each continent was generally positive, with the exception of Africa. Africa has the second largest population worldwide, but there has been little research on SUHIs, mainly in the Nile and delta regions [66,67]. This may be due to the low rate of urbanization in Africa, where there is no significant difference in temperature between urban and rural areas [68], and therefore, the heat island effect is less obvious and less of a concern.

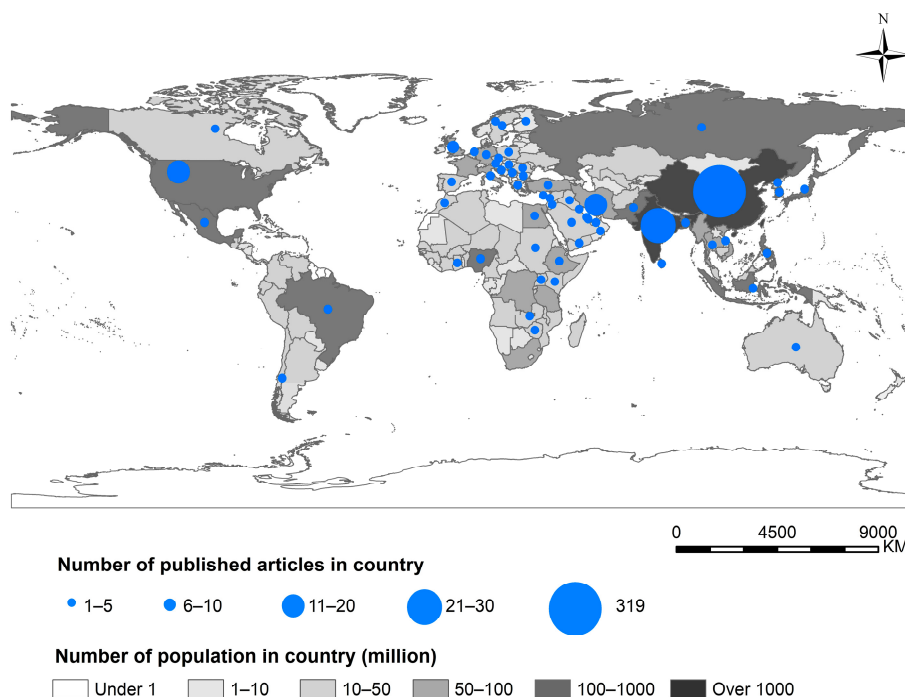


Figure 3. Number of published articles and populations at the country level.

With respect to the application of different research methods in various countries worldwide (Figure 4), SUHI studies are mainly conducted in Asia, Europe, and North America. The research method using the urban–rural method as the SUHI is the most widely applied in the world [69], with a total of 137 applications. This method has been used more frequently in the United States, India, and England [70–72]. The urban–buffer zone method as SUHI was applied 113 times, mainly in China, the United States, European countries, and Eastern Africa [73–75]. Most articles that used several cities around the world as the scope of the study used the urban–buffer zone method as the main means of calculating the SUHI [34,35,76]. This is because this method expands a certain distance outward from the center of the city, thus, delineating the buffer zone outside the built-up area and minimizing errors among the different cities studied. The LST/BT grading method

is primarily used in China, Iran, and India [77,78]. The urban–field method is mainly used in the plains of China, Korea, and Japan [79,80]. The urban–vegetation method is mainly applied in China, Brazil, and the Philippines [37]. Most of Brazil is covered by Amazon rainforest, and the Philippine archipelago is rich in species of vegetation, with abundant forests and jungles, while southeastern China is also rich in vegetation resources; therefore, the urban–vegetation method can be applied to calculate the SUHII in areas with high vegetation cover. The urban–water body method can generally be applied to study areas with larger lakes to measure the SUHII by comparing the differences in the LST between urban areas and lakes, such as Taihu Lake in Suzhou and Zalew Zegrzyński Lake in Warsaw, Poland [39]. The LCZs method is currently applied mostly to the study of temperature and other broad aspects and less often to the study of the SUHII [81,82]. A variety of SUHI research methods are used in Asia, including China, Iran, and India, whereas authors in Europe and North America prefer to use the urban–rural and urban–buffer zone methods. It is worth noting that the most significant difference between China and other countries is that the URI and UTFVI are heavily used in China, but fewer researchers in other countries use these methods.

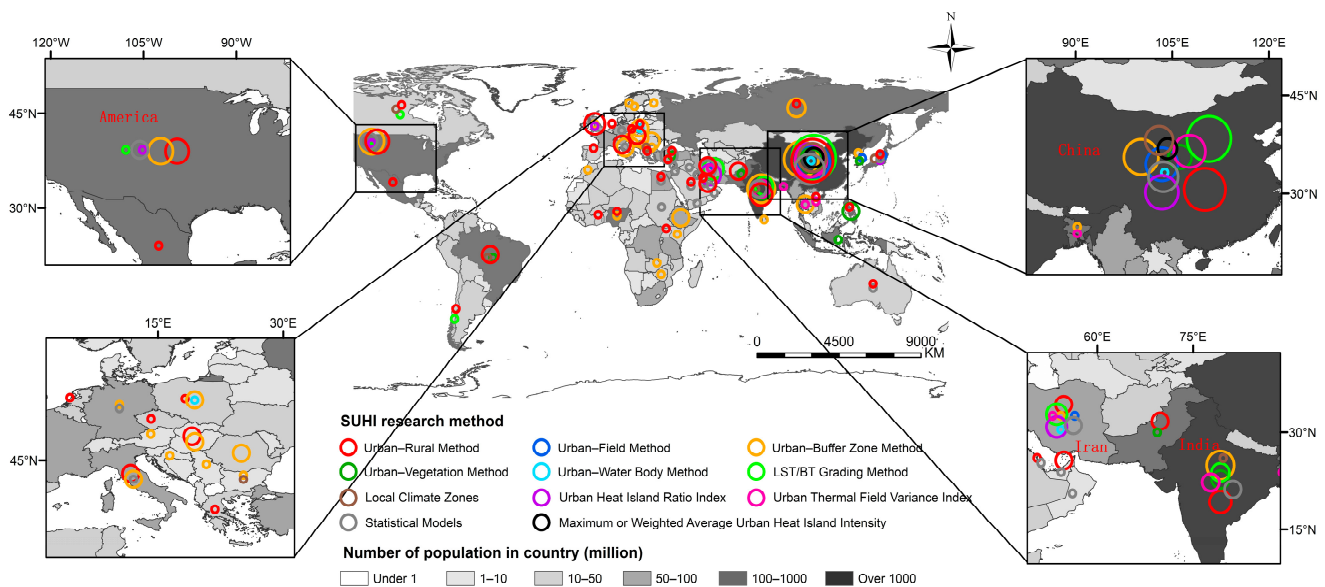


Figure 4. Application of different research methods in different countries.

China is the most studied country in SUHI research, with a frequency of 374 studies, mostly by Chinese academics, and the research range is mainly based in municipal areas and urban agglomerations [83,84], mostly in the Beijing–Tianjin–Hebei (BTH), Yangtze River Delta (YRD), and Pearl River Delta (PRD) agglomerations; Guangdong–Hong Kong–Macao Greater Bay Area (GBA); and provincial capitals. Therefore, in this paper, the application of different research methods in different cities in China is summarized, as shown in Figure 5. With a vast land area, crossing several climatic zones from south to north and complex and diverse land use types, SUHIs have always been the focus of academic research in China. Thirty-five studies were conducted at the national scale [74,85,86]. Among the municipal-scale studies, Beijing was the most frequently researched [87,88], with 50 articles, accounting for 10.3% of the study area. As the capital of China and center of political, cultural, scientific, and technological innovation, Beijing has witnessed radical changes in urban development over the past decades, and the UHI phenomenon has become increasingly serious [8], which has been widely noticed and studied by academics. Additionally, Wuhan and Shanghai were selected as research regions by both domestic and foreign researchers [23,89], accounting for 5.0% and 4.3%, respectively. All these cities are characterized by large resident populations, rapid socioeconomic development, and high urbanization rates.

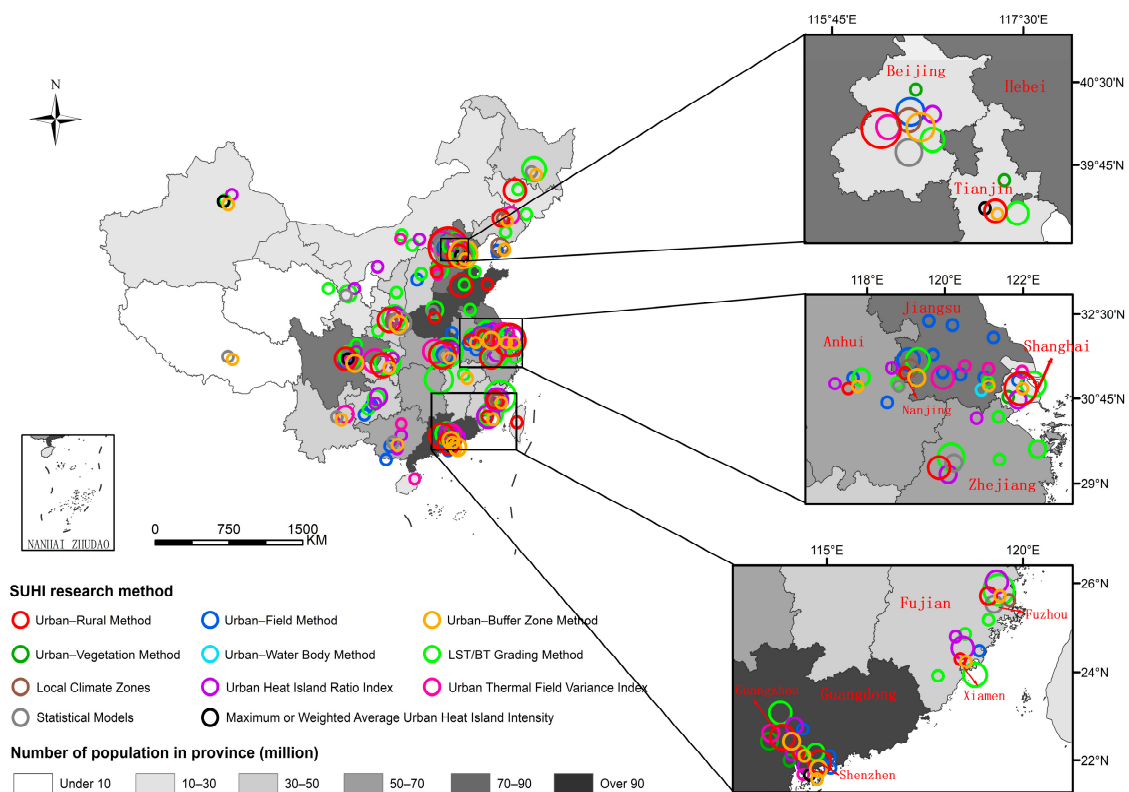


Figure 5. Application of different research methods in different cities in China.

The urban–rural method was applied 59 times, for which Beijing and Shanghai were more frequently used in domestic studies [84,89], accounting for 25.4% and 17.0%, respectively, and the remaining provincial capitals also used this method more frequently [28]. Beijing, Shanghai, and provincial capitals, where the urban core is highly developed in terms of construction, are more prominent in contrast to the rural or suburban areas in terms of urbanization development; thus, using this method in these cities makes it easier to filter out a suitable sample of urban and rural pixels to calculate the SUHII. Research using the urban–field method has mainly been conducted in areas around the middle and lower parts of the YRD and North China Plain [79,90]. These regions have repeatedly been reorganized according to administrative divisions in recent years, resulting in the division of urban and rural areas being limited only to the administrative-division level. However, these areas have smooth surfaces and more croplands around cities; thus, the SUHII can be calculated using this method. The city with the most applied urban–buffer zone method was Beijing, especially within its fifth ring [91], because it has a layout of concentric circles, with the core of the city expanding outward to establish a buffer zone, which can be better spread to all areas. The LST/BT grading method is the most common method for describing the SUHIs in various cities because it is simpler to calculate and more universal. This method grades the LST of a region and defines high-temperature areas as heat island areas. It can also reflect the spatiotemporal evolution patterns of a SUHI using the LST in different periods, which is widely used in studies conducted at the municipal scale, particularly in Fuzhou, Wuhan, Changsha, Hangzhou, and other regions, with high application frequency [41,92]. The URI method often follows the LST/BT grading method [93], because it describes the proportion and intensity of each class. The larger the index, the more serious the UHI, and this method further illustrates the SUHII based on the LST/BT grading method. The city where the UTFVI was most applied was Chongqing, and it was generally applied more in the southern region than in the northern region [94]. Other methods are used less frequently, and they are applied in more dispersed cities; thus, no obvious patterns can currently be analyzed.

Further, we selected the top 14 cities (seven megacities: Shanghai, Beijing, Shenzhen, Chongqing, Guangzhou, Chengdu, and Tianjin; seven supercities: Wuhan, Dongguan, Xi'an, Hangzhou, Foshan, Nanjing, and Shenyang) in terms of the latest city ratings released by the National Bureau of Statistics to conduct a correlation study between the application of the SUHI method and the research area (Figure 6). Beijing was far ahead in terms of the number of articles published. Although Shanghai, Guangzhou, and Shenzhen are all first-tier cities, they are often classified as urban agglomerations for research because they are in the YRD or PRD agglomeration. Therefore, the number of studies conducted at the municipal scale was low [95,96]. Even though Beijing is part of the BTH agglomeration, its development rate is substantially faster than that of neighboring cities, and most studies have only used Beijing as the research area [40,97]. In contrast, fewer studies have used Foshan and Dongguan city as research areas, mainly because they belong to the PRD agglomeration and GBA, where the integrated development of city agglomerations makes many researchers choose urban agglomeration as a research scale rather than individual cities [98,99]. The highest number of SUHI studies among the megacities was in Wuhan [30], probably because of the high number of relevant local research institutes, academics, and significant research achievements. In terms of research methods, the most widely used method in Beijing is the urban–rural dichotomy method, which accounts for approximately one-third of the total [8,100]. The urban–buffer zone, urban–field, and statistical models were also applied more frequently [87], but the results of the SUHI vary owing to the method, and the quantitative portrayal of the UHI effect differs somewhat among academics. The application of this method to calculate the SUHI using croplands as rural representative pixels is limited by the topographic conditions in hilly areas, such as in Chongqing and Dongguan; therefore, this method has not been used in these areas. Furthermore, the LCZs method, which emerged in recent years, can quantify the impacts of different urban forms on the UHI effect by correlating the urban form with the UHI. However, this method is currently only applied in Beijing and Nanjing [40] and can be applied to other large cities with greater development in future research to explore the complex relationship between various LCZs and UHIs and provide a reference for more detailed urban planning.

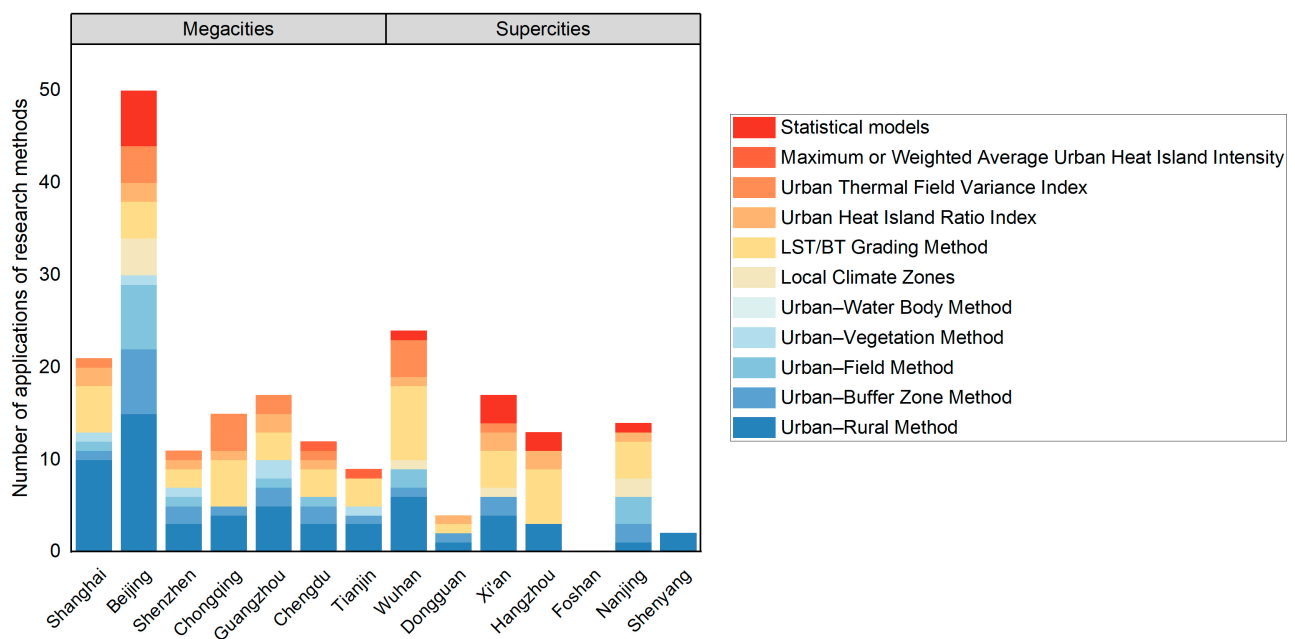


Figure 6. Number of applications of different research methods in megacities and supercities.

6. Discussion

This review compiled and analyzed SUHI research from the last 20 years; however, for the literature search, we only used the CNKI and WOS databases, which may not be comprehensive. Furthermore, the search keywords chosen may have resulted in some articles not being searched, potentially resulting in inaccuracies in the research data and results of this article. These are the limitations of this paper. Furthermore, we discovered that while SUHI research has made significant advances over the last 20 years, there are still several flaws and limitations in the research methodology and data sources that need to be addressed further.

6.1. Limitations of the Research Methods

There are currently several methods for researching the SUHI, and the results vary. Using urban–rural indicators, Haashemi et al. [13] discovered that in semi-arid cities, such as Tehran, with the urban-rural indicator, a surface urban cool island may be observed in daytime while SUHI at nighttime; with other indicators (urban-field and urban-water body method), SUHI can be observed in both day and night. Schwarz et al. [14] quantified SUHIs in the European region using three metrics and discovered that the explanatory power of these models varied significantly. The method of dividing urban and nonurban areas is not clear. For large range studies involving multiple cities, each city varies in size, population density, construction intensity, and land cover type. Therefore, a single study method is not necessarily applicable to all cities. Zhou et al. [101] found that when calculating the SUHI, if the method of dividing a city and other areas is different, the results will change, and even the opposite result of switching from the cold island effect to the heat island effect will occur. Liu et al. [22] estimated the SUHI for 281 Chinese cities using seven methods. The results showed that changing the nonurban references changed the SUHI and the nature of the observed surface thermal island (heat or cold) in 74% and 8% of the cities, respectively. Although some statistical models exist to reduce errors caused by urban–rural divides, many uncertainties remain [50]. As a result, it is critical to carefully select the SUHI research methods for each city. Furthermore, it would be more constructive for SUHI research if a methods system suitable for quantifying the SUHI at various scales worldwide was constructed with different methods selected for diverse research and comparative analyses according to different cities.

6.2. Unbalanced Distribution in the Research Area

On the one hand, as discussed in Section 5.2, SUHI research areas are mainly focused in Asia, especially China and India. However, research in areas such as Africa, South America, and Oceania has been limited. According to Zhou et al. [18], Africa, South America, and India have a high urbanization potential and/or climate sensitivity. And in this century, urban population growth and land expansion are expected to occur primarily in Africa and Asia. This means that SUHIs in these areas necessitate additional research and attention. According to our data, India had the second highest number of SUHI studies, but it was still far behind China. However, India has experienced rapid population growth in recent years, as well as an increase in the frequency of extreme heat events [102,103]. There is no doubt that academics in India must increase the amount of SUHI research. The complexity and diversity of climatic conditions in Africa make studying the impact of climate change on regional SUHI equally important. On the other hand, there are only 14 articles with a global scale (Section 5.2). The majority of research has been conducted at the scale of individual cities or urban agglomerations, with little research conducted at the global and intercontinental levels. This makes obtaining a complete picture of the spatial and temporal variation patterns of SUHIs difficult. The issue of research scope is one that needs to be addressed in the future.

6.3. Lack Impact of LST Data on SUHI Research

The SUHI method mainly depends on the LST obtained from the thermal infrared remote sensing technology; however, it is affected by cloud cover, and the lack of image values seriously restricts the development of SUHI research [104,105]. SUHI is characterized by transient variations, among which diurnal, interlunar, and interannual variations are current research hotspots [106,107]. Therefore, it was necessary to acquire LST images of the study area over multiple periods. If cloud cover causes a lack of values in LST images, it restricts the study of spatiotemporal patterns and trends in SUHIs. Currently, many academics are working to develop methods to reduce the impact of cloud cover on LST retrieval. On the one hand, homomorphic filtering [108] and wavelet transform methods [109] eliminate the effects of thin clouds, but these methods are less effective at eliminating thick clouds. On the other hand, integrating multisource remote sensing datasets and replacing images of areas with cloud-covered areas by fusing multitemporal, multispectral, and multiplatform remote sensing images can make up for the shortcomings of single images, but the spatial resolution of the reconstructed LST is low [110]. In summary, although there are methods to reduce the impact of cloud cover on the LST, the computational efficiency and accuracy can be improved. LST retrieval is affected by the satellite orbital reentry period in addition to cloud cover. Most SUHI dynamics research has concentrated on a single time node or typical time nodes in a diurnal and/or seasonal cycle [111]. To address this limitation, Liu et al. [111] combined the annual temperature cycle (ATC) and diurnal temperature cycle (DTC) models to study continuous seasonal/diurnal SUHI in over 2000 cities worldwide. Furthermore, the accuracy of the LST retrieval must be explored. Accuracy verification can be classified into temperature-based methods (T-based), radiation-based methods (R-based), and cross-validation; however, all of these methods have limitations [112]. The accuracy of the LST significantly affects the accuracy of the SUHI. This means that many challenges remain in SUHI research.

6.4. Effect of Thermal Radiation Directionality on LST

Thermal radiation directionality (TRD) is one of the difficulties in the LST retrieval process, which limits the progress of SUHI research [113]. Voogt et al. [114] carried a helicopter with thermal infrared sensors and conducted aerial observations of downtown Vancouver from different viewpoints, finding maximum temperature differences of up to 9 K in an urban area. At present, as there are few satellite remote sensing images of both high temporal and spatial resolutions, and it is difficult to obtain data from large areas for near-ground observation; it is more difficult to observe the same scene from different angles simultaneously. Thus, the existing satellite products cannot meet the demand for high accuracy in LST retrieval, which affects the accuracy of UHI research. Observational experiments and model simulations are the two major current research tools used for the TRD [115,116]. Platform-based observations, such as drones, can generate multi-angle datasets of different surfaces at low cost and in a short amount of time or build a series of models for simulation studies, such as radiative transfer models (RTMs), hybrid models (HMs), 3D models, and kernel drive models (KDMs). However, these research methods have advantages and disadvantages [113]: RTMs require too many input parameters, the computational processes of HMs and 3D models are complex, the development of KDMs is not advanced enough yet, and these models' accuracy needs further validation. The problem of normalizing the angular effect of the LST needs to be further addressed in future research to better promote the UHI.

7. Conclusions

This article reviewed the number of published articles, research methods, and spatial and temporal distribution characteristics of the study area from research over the last 20 years; summarized and analyzed from multiple dimensions; and drew the following conclusions.

The number of studies on SUHIs began to rise rapidly in 2009, which is closely related to global warming and rapid urbanization, and people are highly concerned about the sustainable development of society and enhancement of human well-being; academics all over the world have researched SUHIs from various aspects and perspectives and made significant advancements.

SUHI has been studied using various methods. The temperature dichotomy method is the most widely used method globally in which the urban–rural method is the most widely applied method for the SUHI; however, obtaining accurate definitions of urban and rural areas is one of the main challenges. The LST/BT grading method is widely used in China, and it can be used to quickly identify the spatial and temporal distributions of heat islands in different periods and to compare and analyze their evolutionary characteristics. Additionally, the method is usually combined with URI to quantify the statistics of heat island classes and the SUHI. The application of statistical models is limited by topography, elevation, and other conditions, making it difficult to satisfy the requirements for SUHI comparisons in different cities.

The number of applications of various SUHI research methods was similar to the number of publications on the growth trend over the years, and the research hotspots were concentrated in China, India, Iran, the United States, and Western Europe. Most studies were conducted in municipal areas, mainly those with high levels of economic development, population density, and intensity of urban development and construction. Areas with high levels of urbanization have obvious heat island effects, which are more conducive to the analysis of spatial and temporal patterns and evolutionary characteristics. According to the statistics on the application of different methods in different countries and cities, the urban–rural method is used more frequently worldwide. The urban–field method is mainly applied to plain areas, such as the middle and lower reaches of the YR Plain and North China Plain, as well as plain areas in Korea and Japan, where the coverage by fields is more abundant. Fields are used as a representative pixel of nonurban areas to describe the condition of a SUHI. The urban–vegetation method is mainly applied in regions with high vegetation cover, such as southeastern China and Brazilian tropical rainforests. However, the application patterns of the SUHI research methods in China differ from those in other countries. For instance, the LST/BT grading method is widely used in China and often further quantifies the SUHI intensity using the URI or UTFVI; however, such research methods are rarely used in other countries.

Author Contributions: Conceptualization, J.Z. and L.T.; methodology, J.Z. and L.T.; software, J.Z. and B.S.; validation, J.Z. and L.T.; formal analysis, J.Z. and L.T.; investigation, J.Z., L.T., and B.S.; resources, J.Z. and B.S.; data curation, J.Z.; writing—original draft preparation, J.Z., L.T., and B.S.; writing—review and editing, J.Z. and L.T.; visualization, J.Z. and B.S.; supervision, J.Z. and L.T.; project administration, L.T.; funding acquisition, L.T. All authors have read and agreed to the published version of the manuscript.

Funding: This research was funded by the National Natural Science Foundation of China, grant number: 41801234.

Institutional Review Board Statement: Not applicable.

Informed Consent Statement: Not applicable.

Data Availability Statement: Not applicable.

Conflicts of Interest: The authors declare no conflict of interest.

References

1. Howard, L. *The Climate of London: Deduced from Meteorological Observations Made in the Metropolis and at Various Places around It*; Harvey and Darton: London, UK, 1833; Volume 3.
2. Baqa, M.F.; Lu, L.L.; Chen, F.; Nawaz-ul-Huda, S.; Pan, L.; Tariq, A.; Qureshi, S.; Li, B.; Li, Q. Characterizing spatiotemporal variations in the urban thermal environment related to land cover changes in Karachi, Pakistan, from 2000 to 2020. *Remote Sens.* **2022**, *14*, 2164. [[CrossRef](#)]

3. Si, M.L.; Li, Z.L.; Nerry, F.; Tang, B.; Leng, P.; Wu, H.; Zhang, X.; Shang, G. Spatiotemporal pattern and long-term trend of global surface urban heat islands characterized by dynamic urban-extent method and MODIS data. *ISPRS J. Photogramm.* **2022**, *183*, 321–335. [[CrossRef](#)]
4. Shen, Y.; Zeng, C.; Cheng, Q.; Shen, H.F. Opposite spatiotemporal patterns for surface urban heat island of two “stove cities” in China: Wuhan and Nanchang. *Remote Sens.* **2021**, *13*, 4447. [[CrossRef](#)]
5. Chen, Y.; Shuqing, Z. Diverse seasonal hysteresis of surface urban heat islands across Chinese cities: Patterns and drivers. *Remote Sens. Environ.* **2023**, *294*, 113644. [[CrossRef](#)]
6. Zhou, D.C.; Zhao, S.Q.; Liu, S.G.; Zhang, L.X.; Zhu, C. Surface urban heat island in China’s 32 major cities: Spatial patterns and drivers. *Remote Sens. Environ.* **2014**, *152*, 51–61. [[CrossRef](#)]
7. Tian, P.; Li, J.L.; Cao, L.D.; Pu, R.; Wang, Z.; Zhang, H.; Chen, H.; Gong, H. Assessing spatiotemporal characteristics of urban heat islands from the perspective of an urban expansion and green infrastructure. *Sustain. Cities Soc.* **2021**, *74*, 103208. [[CrossRef](#)]
8. Wang, J.; Zhou, W.Q.; Wang, J. Time-series analysis reveals intensified urban heat island effects but without significant urban warming. *Remote Sens.* **2019**, *11*, 2229. [[CrossRef](#)]
9. Aleksandrowicz, O.; Vuckovic, M.; Kiesel, K.; Mahdavi, A. Current trends in urban heat island mitigation research: Observations based on a comprehensive research repository. *Urban. Clim.* **2017**, *21*, 1–26. [[CrossRef](#)]
10. Vásquez-Álvarez, P.E.; Flores-Vázquez, C.; Cobos-Torres, J.C.; Cobos-Mora, S.L. Urban heat island mitigation through planned simulation. *Sustainability* **2022**, *14*, 8612. [[CrossRef](#)]
11. Yao, Y.; Chen, X.; Qian, J. Research progress on the thermal environment of the urban surfaces. *Acta Ecol. Sin.* **2018**, *38*, 1134–1147. [[CrossRef](#)]
12. Rao, P.K. Remote sensing of urban heat islands from an environmental satellite. *Bull. Am. Meteorol. Soc.* **1972**, *53*, 647–648.
13. Haashemi, S.; Weng, Q.H.; Darvishi, A.; Alavipanah, S. Seasonal variations of the surface urban heat island in a semi-arid city. *Remote Sens.* **2016**, *8*, 17. [[CrossRef](#)]
14. Schwarz, N.; Manceur, A.M. Analyzing the influence of urban forms on surface urban heat islands in Europe. *J. Urban. Plan. Dev.* **2015**, *141*, 11. [[CrossRef](#)]
15. Lu, Y.; He, T.; Xu, X.; Qiao, Z. Investigation the robustness of standard classification methods for defining urban heat islands. *I IEEE J. Sel. Top. Appl. Earth Obs. Remote Sens.* **2021**, *14*, 11386–11394. [[CrossRef](#)]
16. Yuan, Y.F.; Zhai, P.M. Latest understanding of extreme weather and climate events under global warming and urbanization influences. *Trans. Atmos. Sci.* **2022**, *45*, 161–166. [[CrossRef](#)]
17. Lian, X.; Piao, S.L.; Chen, A.P.; Huntingford, C.; Fu, B.J.; Li, L.Z.X.; Huang, J.P.; Sheffield, J.; Berg, A.M.; Keenan, T.F.; et al. Multifaceted characteristics of dryland aridity changes in a warming world. *Nat. Rev. Earth Env.* **2021**, *2*, 232–250. [[CrossRef](#)]
18. Zhou, D.; Xiao, J.; Bonafoni, S.; Berger, C.; Deilami, K.; Zhou, Y.; Frolicking, S.; Yao, R.; Qiao, Z.; Sobrino, J. Satellite remote sensing of surface urban heat islands: Progress, challenges, and perspectives. *Remote Sens.* **2018**, *11*, 48. [[CrossRef](#)]
19. Almeida, C.R.d.; Teodoro, A.C.; Gonçalves, A. Study of the Urban Heat Island (UHI) Using Remote Sensing Data/Techniques: A Systematic Review. *Environments* **2021**, *8*, 105. [[CrossRef](#)]
20. Chen, G.Z.; Li, X.; Liu, X.P.; Chen, Y.M.; Liang, X.; Leng, J.Y.; Xu, X.C.; Liao, W.L.; Qiu, Y.A.; Wu, Q.L.; et al. Global projections of future urban land expansion under shared socioeconomic pathways. *Nat. Commun.* **2020**, *11*, 537. [[CrossRef](#)]
21. Liu, Z.H.; Zhan, W.F.; Bechtel, B.; Voogt, J.; Lai, J.M.; Chakraborty, T.; Wang, Z.H.; Li, M.C.; Huang, F.; Lee, X.H. Surface warming in global cities is substantially more rapid than in rural background areas. *Commun. Earth Environ.* **2022**, *3*, 219. [[CrossRef](#)]
22. Liu, H.M.; He, B.J.; Gao, S.H.; Zhan, Q.M.; Yang, C. Influence of non-urban reference delineation on trend estimate of surface urban heat island intensity: A comparison of seven methods. *Remote Sens. Environ.* **2023**, *296*, 113735. [[CrossRef](#)]
23. Shen, H.F.; Huang, L.W.; Zhang, L.P.; Wu, P.H.; Zeng, C. Long-term and fine-scale satellite monitoring of the urban heat island effect by the fusion of multi-temporal and multi-sensor remote sensed data: A 26-year case study of the city of Wuhan in China. *Remote Sens. Environ.* **2016**, *172*, 109–125. [[CrossRef](#)]
24. Li, Y.Z.; Yin, K.; Zhou, H.X.; Wang, X.L.; Hu, D. Progress in urban heat island monitoring by remote sensing. *Prog. Geogr.* **2016**, *35*, 1062–1074. [[CrossRef](#)]
25. Budhiraja, B.; Gawuc, L.; Agrawal, G. Seasonality of surface urban heat island in Delhi city region measured by local climate zones and conventional indicators. *IEEE J. Sel. Top. Appl. Earth Obs. Remote Sens.* **2019**, *12*, 5223–5232. [[CrossRef](#)]
26. Jiang, S.; Peng, J.; Dong, J.Q.; Cheng, X.Y.; Dan, Y.Z. Conceptual connotation and quantitative characterization of surface urban heat island effect. *Acta Geogr. Sin.* **2022**, *77*, 2249–2265. [[CrossRef](#)]
27. Schwarz, N.; Lautenbach, S.; Seppelt, R. Exploring indicators for quantifying surface urban heat islands of European cities with MODIS land surface temperatures. *Remote Sens. Environ.* **2011**, *115*, 3175–3186. [[CrossRef](#)]
28. Ren, T.; Zhou, W.Q.; Wang, J. Beyond intensity of urban heat island effect: A continental scale analysis on land surface temperature in major Chinese cities. *Sci. Total Environ.* **2021**, *791*, 148334. [[CrossRef](#)]
29. Deng, Y.J.; Kuang, Y.Q.; Huang, F. Research of Urban Heat Island in Guangzhou Based on Landsat/TM Data. *Meteorol. Mon.* **2010**, *36*, 26–30.
30. Gui, X.; Wang, L.C.; Yao, R.; Yu, D.Q.; Li, C.A. Investigating the urbanization process and its impact on vegetation change and urban heat island in Wuhan, China. *Environ. Sci. Pollut. Res.* **2019**, *26*, 30808–30825. [[CrossRef](#)] [[PubMed](#)]
31. Zhang, P.; Imhoff, M.L.; Bounoua, L.; Wolfe, R.E. Exploring the influence of impervious surface density and shape on urban heat islands in the northeast United States using MODIS and Landsat. *Can. J. Remote Sens.* **2012**, *38*, 441–451. [[CrossRef](#)]

32. Chakraborty, T.; Lee, X. A simplified urban-extent algorithm to characterize surface urban heat islands on a global scale and examine vegetation control on their spatiotemporal variability. *Int. J. Appl. Earth Obs. Geoinf.* **2019**, *74*, 269–280. [[CrossRef](#)]
33. Wang, L.Y.; Hou, H.; Weng, J.X. Ordinary least squares modelling of urban heat island intensity based on landscape composition and configuration: A comparative study among three megacities along the Yangtze River. *Sustain. Cities Soc.* **2020**, *62*, 102381. [[CrossRef](#)]
34. Clinton, N.; Gong, P. MODIS detected surface urban heat islands and sinks: Global locations and controls. *Remote Sens. Environ.* **2013**, *134*, 294–304. [[CrossRef](#)]
35. Peng, S.S.; Piao, S.L.; Ciais, P.; Friedlingstein, P.; Oettle, C.; Breon, F.M.; Nan, H.J.; Zhou, L.M.; Myneni, R.B. Surface Urban Heat Island Across 419 Global Big Cities. *Environ. Sci. Technol.* **2012**, *46*, 696–703. [[CrossRef](#)]
36. Ye, C.H.; Liu, Y.H.; Liu, W.D.; Liu, C.; Quan, W.J. Research on urban surface heat environment monitoring indexes and its application. *Meteorol. Sci. Technol.* **2011**, *39*, 95–101. [[CrossRef](#)]
37. Fang, Y.B.; Zhan, W.F.; Huang, F.; Gao, L.; Quan, J.L.; Zou, Z.X. Hourly variation of surface urban heat island over the Yangtze River Delta urban agglomeration. *Adv. Earth Sci.* **2017**, *32*, 187–198. [[CrossRef](#)]
38. Zhou, D.C.; Bonafoni, S.; Zhang, L.X.; Wang, R.H. Remote sensing of the urban heat island effect in a highly populated urban agglomeration area in East China. *Sci. Total Environ.* **2018**, *628–629*, 415–429. [[CrossRef](#)]
39. Gawuc, L.; Struzewska, J. Impact of MODIS Quality Control on Temporally Aggregated Urban Surface Temperature and Long-Term Surface Urban Heat Island Intensity. *Remote Sens.* **2016**, *8*, 374. [[CrossRef](#)]
40. Zhang, Y.T.; Li, D.L.; Liu, L.B.; Liang, Z.; Shen, J.S.; Wei, F.L.; Li, S.C. Spatiotemporal Characteristics of the Surface Urban Heat Island and Its Driving Factors Based on Local Climate Zones and Population in Beijing, China. *Atmosphere* **2021**, *12*, 1271. [[CrossRef](#)]
41. Xiong, Y.; Zhang, F. Thermal environment effects of urban human settlements and influencing factors based on multi-source data: A case study of Changsha city. *Acta Geogr. Sin.* **2020**, *75*, 2443–2458. [[CrossRef](#)]
42. Huang, J.C.; Zhao, X.F.; Tang, L.N.; Qiu, Q.Y. Analysis on spatiotemporal changes of urban thermal landscape pattern in the context of urbanisation: A case study of Xiamen City. *Acta Ecol. Sin.* **2012**, *32*, 622–631. [[CrossRef](#)]
43. Xu, H.Q.; Chen, B.Q. An image processing technique for the study of urban heat island changes using different seasonal remote sensing data. *Remote Sens. Technol. Appl.* **2003**, *18*, 129–133. [[CrossRef](#)]
44. Chen, X.; Zhang, Y.P. Impacts of urban surface characteristics on spatiotemporal pattern of land surface temperature in Kunming of China. *Sustain. Cities Soc.* **2017**, *32*, 87–99. [[CrossRef](#)]
45. Zhang, W.; Chen, W.X. Analysis of winter heat island intensity in Chengdu based on MODIS. *Sci. Technol. Eng.* **2015**, *15*, 197–201. [[CrossRef](#)]
46. Hu, J.; Yang, Y.B.; Zhou, Y.Y.; Zhang, T.; Ma, Z.; Meng, X. Spatial patterns and temporal variations of footprint and intensity of surface urban heat island in 141 China cities. *Sustain. Cities Soc.* **2022**, *77*, 10. [[CrossRef](#)]
47. Weng, Q.H.; Rajasekar, U.; Hu, X.F. Modeling urban heat islands and their relationship with impervious surface and vegetation abundance by using ASTER images. *IEEE Trans. Geosci. Remote Sens.* **2011**, *49*, 4080–4089. [[CrossRef](#)]
48. Liu, F.; Hou, H.; Murayama, Y. Spatial interconnections of land surface temperatures with land cover/use: A case study of Tokyo. *Remote Sens.* **2021**, *13*, 610. [[CrossRef](#)]
49. Li, F.; Sun, W.W.; Yang, G.; Weng, Q.H. Investigating Spatiotemporal Patterns of Surface Urban Heat Islands in the Hangzhou Metropolitan Area, China, 2000–2015. *Remote Sens.* **2019**, *11*, 1553. [[CrossRef](#)]
50. Li, H.D.; Zhou, Y.Y.; Li, X.M.; Meng, L.; Wang, X.; Wu, S.; Sodoudi, S. A new method to quantify surface urban heat island intensity. *Sci. Total Environ.* **2018**, *624*, 262–272. [[CrossRef](#)]
51. Zhang, Y.Z.; Cheng, J. Spatio-Temporal Analysis of Urban Heat Island Using Multisource Remote Sensing Data: A Case Study in Hangzhou, China. *IEEE J.-Stars.* **2019**, *12*, 3317–3326. [[CrossRef](#)]
52. Yao, R.; Wang, L.C.; Huang, X.; Gong, W.; Xia, X.G. Greening in Rural Areas Increases the Surface Urban Heat Island Intensity. *Geophys. Res. Lett.* **2019**, *46*, 2204–2212. [[CrossRef](#)]
53. Niu, L.; Tang, R.L.; Jiang, Y.Z.; Zhou, X.M. Spatiotemporal patterns and drivers of the surface urban heat island in 36 major cities in China: A comparison of two different methods for delineating rural areas. *Sustainability* **2020**, *12*, 478. [[CrossRef](#)]
54. Li, K.N.; Chen, Y.H.; Gao, S.J. Uncertainty of city-based urban heat island intensity across 1112 global cities: Background reference and cloud coverage. *Remote Sens. Environ.* **2022**, *271*, 112898. [[CrossRef](#)]
55. Yao, R.; Wang, L.C.; Huang, X.; Niu, Y.; Chen, Y.S.; Niu, Z. The influence of different data and method on estimating the surface urban heat island intensity. *Ecol. Indic.* **2018**, *89*, 45–55. [[CrossRef](#)]
56. Peres, L.D.; de Lucena, A.J.; Rotunno, O.C.; Franca, J.R.D. The urban heat island in Rio de Janeiro, Brazil, in the last 30 years using remote sensing data. *Int. J. Appl. Earth Obs.* **2018**, *64*, 104–116. [[CrossRef](#)]
57. Wei, C.Z.; Chen, W.; Lu, Y.; Blaschke, T.; Peng, J.; Xue, D. Synergies between urban heat island and urban heat wave effects in 9 global mega-regions from 2003 to 2020. *Remote Sens.* **2022**, *14*, 21. [[CrossRef](#)]
58. Imhoff, M.L.; Zhang, P.; Wolfe, R.E.; Bounoua, L. Remote sensing of the urban heat island effect across biomes in the continental USA. *Remote Sens. Environ.* **2010**, *114*, 504–513. [[CrossRef](#)]
59. Shahfahad; Naikoo, M.W.; Naikoo, M.W.; Towfiqul Islam, A.R.M.; Mallick, J.; Rahman, A. Land use/land cover change and its impact on surface urban heat island and urban thermal comfort in a metropolitan city. *Urban Clim.* **2022**, *41*, 101052. [[CrossRef](#)]

60. Hu, J.; Yang, Y.B.; Pan, X.; Zhu, Q.; Zhan, W.; Wang, Y.; Ma, W.; Su, W. Analysis of the spatial and temporal variations of land surface temperature based on local climate zones: A case study in Nanjing, China. *IEEE J. Sel. Top. Appl. Earth Obs. Remote Sens.* **2019**, *12*, 4213–4223. [[CrossRef](#)]
61. Amorim, M.C.D.T.; Dubreuil, V.; Amorim, A.T. Day and night surface and atmospheric heat islands in a continental and temperate tropical environment. *Urban Clim.* **2021**, *38*, 100918. [[CrossRef](#)]
62. Han, J.; Liu, J.; Liu, L.; Ye, Y. Spatiotemporal changes in the urban heat island intensity of distinct local climate zones: Case study of Zhongshan District, Dalian, China. *Complexity* **2020**, *2020*, 8820338. [[CrossRef](#)]
63. Yang, K.; Zhou, T.; Wang, C.L.; Wang, Z.L.; Han, Q.L.; Tao, F. RSEDM: A New Rotational-Scan Exponential Decay Model for Extracting the Surface Urban Heat Island Footprint. *Remote Sens.* **2022**, *14*, 20. [[CrossRef](#)]
64. Zhang, P.; Imhoff, M.L.; Wolfe, R.E.; Bounoua, L. Characterizing urban heat islands of global settlements using MODIS and nighttime lights products. *Can. J. Remote Sens.* **2010**, *36*, 185–196. [[CrossRef](#)]
65. Stewart, I.D.; Oke, T.R. Local climate zones for urban temperature studies. *Bull. Am. Meteorol. Soc.* **2012**, *93*, 1879–1900. [[CrossRef](#)]
66. Hereher, M.; Eissa, R.; Alqasemi, A.; El Kenawy, A.M. Assessment of air pollution at Greater Cairo in relation to the spatial variability of surface urban heat island. *Environ. Sci. Pollut. Res.* **2022**, *29*, 21412–21425. [[CrossRef](#)]
67. Athukorala, D.; Murayama, Y. Urban Heat Island Formation in Greater Cairo: Spatio-Temporal Analysis of Daytime and Nighttime Land Surface Temperatures along the Urban-Rural Gradient. *Remote Sens.* **2021**, *13*, 1396. [[CrossRef](#)]
68. Gizelis, T.I.; Pickering, S.; Urdal, H. Conflict on the urban fringe: Urbanization, environmental stress, and urban unrest in Africa. *Polit. Geogr.* **2021**, *86*, 102357. [[CrossRef](#)]
69. Yao, R.; Wang, L.C.; Wang, S.Q.; Wang, L.Z.; Wei, J.; Li, J.L.; Yu, D.Q. A detailed comparison of MYD11 and MYD21 land surface temperature products in mainland China. *Int. J. Digit. Earth* **2020**, *13*, 1391–1407. [[CrossRef](#)]
70. Manoli, G.; Faticchi, S.; Bou-Zeid, E.; Katul, G.G. Seasonal hysteresis of surface urban heat islands. *Proc. Natl. Acad. Sci. USA* **2020**, *117*, 7082–7089. [[CrossRef](#)]
71. Feng, J.L.; Cai, X.M.; Chapman, L. Impact of atmospheric conditions and levels of urbanization on the relationship between nocturnal surface and urban canopy heat islands. *Q. J. Roy. Meteor. Soc.* **2019**, *145*, 3284–3299. [[CrossRef](#)]
72. Mukherjee, S.; Joshi, P.K.; Garg, R.D. Analysis of urban built-up areas and surface urban heat island using downscaled MODIS derived land surface temperature data. *Geocarto Int.* **2017**, *32*, 900–918. [[CrossRef](#)]
73. Venter, Z.S.; Chakraborty, T.; Lee, X.H. Crowdsourced air temperatures contrast satellite measures of the urban heat island and its mechanisms. *Sci. Adv.* **2021**, *7*, eabb9569. [[CrossRef](#)] [[PubMed](#)]
74. Yao, R.; Wang, L.C.; Huang, X.; Liu, Y.T.; Niu, Z.G.; Wang, S.Q.; Wang, L.Z. Long-term trends of surface and canopy layer urban heat island intensity in 272 cities in the mainland of China. *Sci. Total Environ.* **2021**, *772*, 145607. [[CrossRef](#)]
75. Raj, S.; Paul, S.K.; Chakraborty, A.; Kuttippurath, J. Anthropogenic forcing exacerbating the urban heat islands in India. *J. Environ. Manag.* **2020**, *257*, 110006. [[CrossRef](#)] [[PubMed](#)]
76. Du, H.L.; Zhan, W.F.; Liu, Z.H.; Li, J.F.; Li, L.; Lai, J.M.; Miao, S.Q.; Huang, F.; Wang, C.G.; Wang, C.L.; et al. Simultaneous investigation of surface and canopy urban heat islands over global cities. *Isprs J. Photogramm.* **2021**, *181*, 67–83. [[CrossRef](#)]
77. Wang, Y.A.; Yi, G.H.; Zhou, X.B.; Zhang, T.B.; Bie, X.J.; Li, J.J.; Ji, B.W. Spatial distribution and influencing factors on urban land surface temperature of twelve megacities in China from 2000 to 2017. *Ecol. Indic.* **2021**, *125*, 107533. [[CrossRef](#)]
78. Firozjaei, M.K.; Fatholouloumi, S.; Kiavarz, M.; Arsanjani, J.J.; Alavipanah, S.K. Modelling surface heat island intensity according to differences of biophysical characteristics: A case study of Amol city, Iran. *Ecol. Indic.* **2020**, *109*, 105816. [[CrossRef](#)]
79. Chen, S.Z.; Yu, Z.W.; Liu, M.; Da, L.J.; Hassan, M.F.U. Trends of the contributions of biophysical (climate) and socioeconomic elements to regional heat islands. *Sci. Rep.* **2021**, *11*, 12696. [[CrossRef](#)]
80. Choi, Y.Y.; Suh, M.S.; Park, K.H. Assessment of Surface Urban Heat Islands over Three Megacities in East Asia Using Land Surface Temperature Data Retrieved from COMS. *Remote Sens.* **2014**, *6*, 5852–5867. [[CrossRef](#)]
81. Alexander, P.J.; Mills, G. Local Climate Classification and Dublin’s Urban Heat Island. *Atmosphere* **2014**, *5*, 755–774. [[CrossRef](#)]
82. Molnar, G.; Gyongyosi, A.Z.; Gal, T. Integration of an LCZ-based classification into WRF to assess the intra-urban temperature pattern under a heatwave period in Szeged, Hungary. *Theor. Appl. Climatol.* **2019**, *138*, 1139–1158. [[CrossRef](#)]
83. Wang, Z.A.; Meng, Q.Y.; Allam, M.; Hu, D.; Zhang, L.L.; Menenti, M. Environmental and anthropogenic drivers of surface urban heat island intensity: A case-study in the Yangtze River Delta, China. *Ecol. Indic.* **2021**, *128*, 107845. [[CrossRef](#)]
84. Hu, Y.H.; Hou, M.T.; Jia, G.S.; Zhao, C.L.; Zhen, X.J.; Xu, Y.H. Comparison of surface and canopy urban heat islands within megacities of eastern China. *Isprs J. Photogramm.* **2019**, *156*, 160–168. [[CrossRef](#)]
85. Lai, J.M.; Zhan, W.F.; Huang, F.; Voogt, J.; Bechtel, B.; Allen, M.; Peng, S.S.; Hong, F.L.; Liu, Y.X.; Du, P.J. Identification of typical diurnal patterns for clear-sky climatology of surface urban heat islands. *Remote Sens. Environ.* **2018**, *217*, 203–220. [[CrossRef](#)]
86. Li, K.N.; Chen, Y.H.; Wang, M.J.; Gong, A. Spatial-temporal variations of surface urban heat island intensity induced by different definitions of rural extents in China. *Sci. Total Environ.* **2019**, *669*, 229–247. [[CrossRef](#)]
87. Qiao, Z.; Wu, C.; Zhao, D.Q.; Xu, X.L.; Yang, J.L.; Feng, L.; Sun, Z.Y.; Liu, L. Determining the Boundary and Probability of Surface Urban Heat Island Footprint Based on a Logistic Model. *Remote Sens.* **2019**, *11*, 1368. [[CrossRef](#)]
88. Meng, Q.Y.; Zhang, L.L.; Sun, Z.H.; Meng, F.; Wang, L.; Sun, Y.X. Characterizing spatial and temporal trends of surface urban heat island effect in an urban main built-up area: A 12-year case study in Beijing, China. *Remote Sens. Environ.* **2018**, *204*, 826–837. [[CrossRef](#)]

89. Huang, F.; Zhan, W.F.; Voogt, J.; Hu, L.Q.; Wang, Z.H.; Quan, J.L.; Ju, W.M.; Guo, Z. Temporal upscaling of surface urban heat island by incorporating an annual temperature cycle model: A tale of two cities. *Remote Sens. Environ.* **2016**, *186*, 1–12. [[CrossRef](#)]
90. Liu, Y.H.; Fang, X.Y.; Xu, Y.M.; Zhang, S.; Luan, Q.Z. Assessment of surface urban heat island across China's three main urban agglomerations. *Theor. Appl. Climatol.* **2018**, *133*, 473–488. [[CrossRef](#)]
91. Li, J.Y.; Sun, R.H.; Liu, T.; Xie, W.; Chen, L.D. Prediction models of urban heat island based on landscape patterns and anthropogenic heat dynamics. *Landscape Ecol.* **2021**, *36*, 1801–1815. [[CrossRef](#)]
92. Lin, R.P.; Qi, X.H.; Ye, S.L. Spatial-temporal characteristics of urban heat islands and driving mechanisms in a coastal valley-basin city: A case study of Fuzhou City. *Acta Ecol. Sin.* **2017**, *37*, 294–304. [[CrossRef](#)]
93. Li, L.; Xu, H.Q. Urban Expansion and Thermal Environment Changes in Hangzhou City of East China. *Remote Sens. Technol. Appl.* **2014**, *29*, 264–272.
94. Luo, X.B.; Chen, D.; Liu, M.H.; Liu, Q. Application Research on Monitor of Heat Island Effect in Chongqing Based on HJ-1B/IRS. *J. Geo-Inf. Sci.* **2011**, *13*, 833–839. [[CrossRef](#)]
95. Shen, Z.C.; Xu, X.L. Influence of the Economic Efficiency of Built-Up Land (EEBL) on Urban Heat Islands (UHIs) in the Yangtze River Delta Urban Agglomeration (YRDUA). *Remote Sens.* **2020**, *12*, 3944. [[CrossRef](#)]
96. Yao, R.; Wang, L.C.; Huang, X.; Chen, J.P.; Li, J.R.; Niu, Z.G. Less sensitive of urban surface to climate variability than rural in Northern China. *Sci. Total Environ.* **2018**, *628–629*, 650–660. [[CrossRef](#)]
97. Fu, P.; Weng, Q.H. Consistent land surface temperature data generation from irregularly spaced Landsat imagery. *Remote Sens. Environ.* **2016**, *184*, 175–187. [[CrossRef](#)]
98. Lin, Y.; Wang, Z.F.; Jim, C.Y.; Li, J.B.; Deng, J.S.; Liu, J.G. Water as an urban heat sink: Blue infrastructure alleviates urban heat island effect in mega-city agglomeration. *J. Clean. Prod.* **2020**, *262*, 1411. [[CrossRef](#)]
99. Li, J.F.; Wang, F.F.; Fu, Y.C.; Guo, B.Y.; Zhao, Y.L.; Yu, H.F. A Novel SUHI Referenced Estimation Method for Multicenters Urban Agglomeration using DMSP/OLS Nighttime Light Data. *IEEE J.-Stars.* **2020**, *13*, 1416–1425. [[CrossRef](#)]
100. Zhong, C.; Chen, C.; Liu, Y.; Gao, P.; Li, H. A Specific Study on the Impacts of PM2.5 on Urban Heat Islands with Detailed In Situ Data and Satellite Images. *Sustainability* **2019**, *11*, 7075. [[CrossRef](#)]
101. Zhou, D.C.; Zhao, S.Q.; Zhang, L.X.; Sun, G.; Liu, Y.Q. The footprint of urban heat island effect in China. *Sci. Rep.* **2015**, *5*, 11160. [[CrossRef](#)]
102. Shastri, H.; Barik, B.; Ghosh, S.; Venkataraman, C.; Sadavarte, P. Flip flop of Day-night and Summer-Winter Surface Urban Heat Island Intensity in India. *Sci. Rep.* **2017**, *7*, 40178. [[CrossRef](#)] [[PubMed](#)]
103. Halder, B.; Bandyopadhyay, J.; Banik, P. Monitoring the effect of urban development on urban heat island based on remote sensing and geo-spatial approach in Kolkata and adjacent areas, India. *Sustain. Cities Soc.* **2021**, *74*, 10318. [[CrossRef](#)]
104. Weng, Q.H.; Fu, P. Modeling annual parameters of clear-sky land surface temperature variations and evaluating the impact of cloud cover using time series of Landsat TIR data. *Remote Sens. Environ.* **2014**, *140*, 267–278. [[CrossRef](#)]
105. Liao, Y.S.Y.; Shen, X.; Zhou, J.; Ma, J.; Zhang, X.D.; Tang, W.B.; Chen, Y.R.; Ding, L.R.; Wang, Z.W. Surface urban heat island detected by all-weather satellite land surface temperature. *Sci. Total Environ.* **2022**, *811*, 151405. [[CrossRef](#)] [[PubMed](#)]
106. Chang, Y.; Xiao, J.F.; Li, X.X.; Zhou, D.C.; Wu, Y.P. Combining GOES-R and ECOSTRESS land surface temperature data to investigate diurnal variations of surface urban heat island. *Sci. Total Environ.* **2022**, *823*, 153652. [[CrossRef](#)]
107. Li, H.D.; Zhou, Y.Y.; Jia, G.S.; Zhao, K.G.; Dong, J.W. Quantifying the response of surface urban heat island to urbanization using the annual temperature cycle model. *Geosci. Front.* **2022**, *13*, 101141. [[CrossRef](#)]
108. Li, G.; Yan, W.N.; Weng, T. A method of removing thin cloud in remote sensing image based on the homomorphic filter algorithm. *Sci. Surv. Mapp.* **2007**, *32*, 47–48.
109. Zhang, B.; Ji, H.M.; Shen, Q. Wavelet-based Cloud Removal from High-resolution Remote Sensing Data: An Experiment with QuickBird Imagery. *Remote Sens. Inf.* **2011**, *3*, 38–43. [[CrossRef](#)]
110. Chen, D.; Wu, W.B.; Lu, M.; Hu, Q.; Zhou, Q.B. Progresses in land cover data reconstruction method based on multi-source data fusion. *Chin. J. Agric. Resour. Reg. Plan.* **2016**, *37*, 62–70. [[CrossRef](#)]
111. Liu, Z.H.; Zhan, W.F.; Lai, J.M.; Bechtel, B.; Lee, X.H.; Hong, F.L.; Li, L.; Huang, F.; Li, J.F. Taxonomy of seasonal and diurnal clear-sky climatology of surface urban heat island dynamics across global cities. *Isprs J. Photogramm.* **2022**, *187*, 14–33. [[CrossRef](#)]
112. Li, Z.L.; Duan, S.B.; Tang, B.H.; Wu, H.; Ren, H.Z.; Yan, G.J.; Tang, R.L.; Len, P. Review of methods for land surface temperature derived from thermal infrared remotely sensed data. *Natl. Remote Sens. Bull.* **2016**, *20*, 899–920. [[CrossRef](#)]
113. Cao, B.; Liu, Q.H.; Du, Y.M.; Roujean, J.L.; Gastellu-Etchegorry, J.P.; Trigo, I.F.; Zhan, W.F.; Yu, Y.Y.; Cheng, J.; Jacob, F.; et al. A review of earth surface thermal radiation directionality observing and modeling: Historical development, current status and perspectives. *Remote Sens. Environ.* **2019**, *232*, 111304. [[CrossRef](#)]
114. Voogt, J.A.; Oke, T.R. Thermal remote sensing of urban climates. *Remote Sens. Environ.* **2003**, *86*, 370–384. [[CrossRef](#)]

115. Cao, B.; Roujean, J.L.; Gastellu-Etchegorry, J.P.; Liu, Q.H.; Du, Y.M.; Lagouarde, J.P.; Huange, H.G.; Li, H.; Bian, Z.J.; Hu, T.; et al. A general framework of kernel-driven modeling in the thermal infrared domain. *Remote Sens. Environ.* **2021**, *252*, 112157. [[CrossRef](#)]
116. Lian, J.; Sun, H.; Lin, Q.; Cao, X.; Li, C.; Huang, H. Field observations of background thermal radiation directionality in natural forests. *Natl. Remote Sens. Bull.* **2017**, *21*, 365–374. [[CrossRef](#)]

Disclaimer/Publisher’s Note: The statements, opinions and data contained in all publications are solely those of the individual author(s) and contributor(s) and not of MDPI and/or the editor(s). MDPI and/or the editor(s) disclaim responsibility for any injury to people or property resulting from any ideas, methods, instructions or products referred to in the content.